NUMERICAL AND EXPERIMENTAL ANALYSIS OF TRANSIENT 2D FLOW AROUND SHIP SPOILER

التحليل الحسابى و التجريبى للسريان الوقتى ثنائى الأبعاد حول الزائدة الجنيحية لسفينة

Nabil H. Mostafa
Mechanical Power Department, College of Engineering
Zagazig University, Zagazig, 44519, Egypt.
Tel: +[20] 50 2334688 Fax: +[20] 50 2331911
E-mail: nmostafa@egyptnetwork.com

خلاصه

يتناول هذا البحث التحليل الحسابى و التجريبى للسريان ثنائى الأبعاد حول الزائدة الجنيحية لسفينة وذلك عند حقن هواء خلف هذه الزائدة الجنيحية التي تم إلصاقها على السطح السفلى لغاطس السفينة أو على مسافه منها. و تستخدم هذه الطريقه للتحكم فى الحركة الإهتزازية الرأسية (الترجح) والدوارة (العطوف) وسرعة السفينة مع الحقن بواسطة غاز العادم. إن القوى والعزم التى تنشأ على السطح السفلى الغاطس للسفينة تعتمد على درجة ميل الزوائد الجنيحية وطولها ووضعها بالنسبة لمركز كتلة السفينة.

ولتحسين فهم العوامل التي تؤثر فى مجال السريان حول هذة الزوائد الجنيحية تم عمليا تصوير ونمذجة مجال السريان حول هذة الزوائد الجنيحية لدراسه تاثير زاويا ميلها المختلفة و مواضع حقن الهواء المختلفة بالنسبه لها. و تم استخدام برنامج حسابى لحل معادلات نافير استوكس فى اتجاهين لنمذجة مجال السريان ثنائى الطور حول الزوائد الجنيحية للسفينة مع إستخدام طريقة المحاكاة للسطح الحر بطريقه البناء القطعى الخطى الثنكى للسطح البينى. تم تمثيل المعادلات الحاكمة على شبكة منشأة باستخدام نظام فرق الإختلاف المضاد للاتجاة. وفى تلك الظروف المختلفة تم حساب شكل الفقاعة ومجال السريان ثنائى الأبعاد حول جسم الزائده الجنيحية واختلافات الضغط على إمتداد مسار المائع لهذة الزائده الجنيحية. و لقد تم استخدام كاميرا فديو لتسجيل مجال السريان حول الزائده فى الحالات و الأزمنه المختلفه. كان عدد فرود يساوى ١,٦ بناء على طول الزائده. أظهرت النتائج العمليه و الحسابيه تطابق جيد و خاصه فى حاله الزائده الجنيحيه ذات ميل ٩٠ ° أما فى حاله الزائده الجنيحيه ذات ميل ٤٥ ° فقد أظهرت النتائج العمليه ان الفقاعه تملأ الفراغ بينها وبين السطح السفلى للسفينه. ذلك الفرق قد يكون نتيجه أن الحسابات تمت فى اتجاهين فقط. و نتيجه لذلك فقد عزل طبقه بين سطح السفينه و الفقاعه. فى حاله الزائده الجنيحيه ذات ميل ٤٥ ° تحدث دوامه داخل الفقاعه و تكون الفقاعه اطول مما أعطى ضغط منخفض على مساحه أكبر. و لذلك فإن العزم الناشئ حول مركز تثبيت الزائده الجنيحيه ذات ميل ٤٥ ° يماثل سبع مرات فى حاله ميلها بمقدار ٩٠ ° . إن الحقن المزدوج بجانب الزائده و على مسافه تساوى طولها الافقى جعلت الفقاعه اكثر اتزانا و زادت العزم حول مركز الزائده بمقدار ٧,٩ و ١٧,٨ ضعفا بعد زمن ١,٢ و٢ ثانيه على التتابع عن حاله ميلها بمقدار ٩٠ °. و بناء على ذلك فان تغيير وضع الزوائد الجنيحية وزاوية ميلها تغير شكل الفقاعه و الضغوط حولها مما يساعد على التحكم فى الحركة الإهتزازية الرأسية والدوارة وسرعة السفينة.

ABSTRACT

An experimental analysis and numerical computation were conducted for flow around ship spoiler mounted at the bottom of the ship and subjected to air injection. The air was injected beside the spoiler and at a distance equals the spoiler length to stabilize cavities behind spoilers. This system was proposed to control the roll, pitch motion and speed of the

Accepted March 23, 2003

ship, with injecting exhaust gas behind spoilers. The forces and moments acting on the ship's bottom depend on spoilers' inclination, extensions and positions relative to the ship's center of mass.

To improve the understanding of the parameters affecting the flow field around such spoiler, experimental images of bubble formation are triggered and compared with the computed flow field at different spoiler inclination angle, and air injection position. Two-dimensional Navier-Stokes code is used to model the two-phase flow field around a ship spoiler with the free surface simulation in Piecewise Linear Interface Construction (PLIC) method. The governing equations are discretized on a structured grid using an upwind difference scheme. For different conditions, the bubbles shape, the two-dimensional flowfield around the spoiler body and the pressure variation on the wake of the spoiler body are computed.

Flow field and bubble formation around the spoiler are recorded experimentally at different condition and time sequence with scientific video camera. The Froude number was about 1.6 based on spoiler length. The computational and experimental results show that there is a good matching of bubble formation in the spoiler with 90°, but in the condition of 45° the experimental images show that bubble filled the space between the bubble and the body of the ship. This is may be due to the two-dimension computational model consideration. So, a water layer was isolated between the bubble and the ship body. In the case of spoiler with 45° inclination angle, the flow is circulated inside the bubble. The bubble shape is longer which gives more negative pressure on larger area. The moment around the 45° spoiler fixation point is seven times of that around the 90° spoiler. In double injection condition beside and at a distance equal the horizontal spoiler length downstream the spoiler, the bubbles are more stable and the moment is higher by 7.9 and 17.8 times after 1.2 and 2 seconds, respectively, than that around the 90° spoiler. Thus, changing inclination spoiler angle and position relative to injection angle will give different bubble shapes which give different forces to control the roll, pitch motion and speed of the ship.

KEYWORDS
Ship, Spoiler, Cavitation, Hydrofoils, Free surface, Two-Phase flows.

NOMENCLATURE

C_∞	upstream velocity	m/s
$\vec{C}$	the local velocity vector in cell c	
d_c	the local cell "dimension" (or length- scale)	
d_p	water tunnel depth	m
dx	element in X direction	m
ds	surface element	m^2
F	liquid volume fraction	
F_r	Froude number, $C/(gL)^{0.5}$	
L	spoiler length	m
P	fluid static pressure	N/m^2
P_t	total pressure	N/m^2
Δt	physical time step	s
Δt_c	the maximum time step that can be taken in cell c	s
u,v,w	velocity in x, y, w respectively	m/s
V_{cut}	the volume of the cell truncated by the cutting plane	m^3
V_c	the volume of the whole cell	m^3

GREEK LETTERS

ϕ	the volume- averaged quantity	m^3
θ	spoiler inclination angle	degree
ρ	density	kg/m^3
σ	the surface tension between the two fluids	N/m
τ	tangential force	N

SUFFIXES

1 the value of the fluid property (air)
2 the value of the fluid property (water)

ABBREVIATION

VOF Volume- Of- Fluid
SLIC Single Line Interface Construction Method
PLIC Piecewise Linear Interface Construction Method
MURI Multi Universities Researches Interactive projects

1. Introdnction

A system of spoilers is mounted at the bottom of the ship. They can be classified into bow spoilers and stern spoilers as shown in Fig. 1. The bow spoilers consist of an even number of sections arranged port and starboard forward of the center of mass of the ship. The stern spoilers consist of an even number of sections arranged port and starboard attached to the ship's transom or transom plate. Hull-mounted cavitating spoilers have been shown, at the Krylov Shipbuilding Research Institute (Russia), to be an effective means for motion reduction in high-speed displacement-hull vessels. The specific design details of the Russian system are not available. Their results, quoted by Soper, et al., 1998 show that by appropriately choosing the number, extension, and distribution of the spoilers, one can achieve an optimal trim of the ship over the whole speed range and a reduction in the ship motion when moving in waves. Roll reduction by a factor of 2 to 5 depending on the sea state. Pitch reduction by a factor of 1.2 to 1.5 depending on the sea state. An increase in the efficiency and hence the speed are by a factor of 10% to 20%. Under "MURI" research project, a theoretical investigation of the effectiveness and design of such a system has been undertaken by Soper, et al., 1998. They used the panel method by developing a two-dimensional quasi-steady numerical local model for the fixed-cavitation region. The computational-fluid-dynamic boundary-element model is based on a distributed-vorticity potential-flow form. The steady-flow streamlines are determined via an iterative approach that converges to a pre-specified level of accuracy. The cavity shape and quasi-steady hydrodynamic forces have been generated over a wide range of forward-speed/cavity-pressure and spoiler-projection-angle parameter values. Owis, et al., 2000, developed a code of Navier-Stokes equation with cavitation procedure function of local pressure and density to solve the same problem.

There is no unique definition of the interface between two phase flow. The cavitation phenomenon depends on the local pressure and density, Mostafa (2001). The cavitation phenomenon, which generated in the case of ship spoiler problem have different reasons. It depends on other parameters as spoiler geometry, location of air injection and air pressure. The basis of the free surface simulation is the Volume- Of- Fluid (VOF) method, which published in an early form by (Hirt and Nichols, 1981), is recently developed by (Rider, et al., 1995). In upwind scheme with the Single Line Interface Construction (SLIC) method, (Noh and Woodward, 1976), the fluid surface is assumed to be parallel to the currently selected cell face, with the relative position of the second fluid depends on the flow direction

and the upstream or downstream value of liquid volume fraction, F. In the Piecewise Linear Interface Construction (PLIC) with upwind scheme, (Kothe, et al., 1996), the liquid- gas interface is assumed to be planar and allowed to take any orientation within the cell, and will therefore generally have the shape of an arbitrary polygonal shape. So, PLIC is more accurate method. The free surface simulation computes the mixture of two incompressible, immiscible fluids, including the effects of surface tensions. The relative mixture of the two fluids within the problem domain is tracked in terms of a secondary fluid volume fraction, F, which, by definition, ranges between 0 and 1. Thus, the strength of the free surface simulation can model the injection of one fluid into the second fluid with arbitrary immiscible fluid- fluid interfaces, which, includes two fluids with very high density ratio, such as air and water.

The objectives of this paper are to study the flow around ship spoiler experimentally and computationally. Experimental images of bubble formation for such spoiler are triggered and compared with the computed flow field and bubble formation at different spoiler inclination angle, and air injection position. The model computes two phase flow field around ship spoiler using two-dimensional Navier-Stokes equation with the free surface simulation using PLIC method. The study included the variation of phenomenon with time. From the pressure variation on the wake of the spoiler body the moment around spoiler fixation will be determined which affect the roll, pitch and speed of the ship.

2. Theory background

The characterizing feature of the VOF methodology is that the distribution of the second fluid (e. g. water) in the computational grid is accounted for using a single scalar field variable, F. Flow field and distribution of F is determined by solving the passive transport equation

$$\frac{\partial F}{\partial t} + \nabla \bullet \vec{C}_c F = 0 \qquad (1)$$

This equation must be solved together with the fundamental equations of conservation of mass and momentum in order to achieve computational coupling between the velocity field solution and the liquid distribution. This requires three related actions: compute mixture properties, reconstruct the fluid- fluid interface in each cell and determine the contribution of the secondary fluid flux. The average value of any volume specific quantity, ϕ, in a computational cell can be computed from the value of F in accordance with

$$\phi = F\phi_2 + (1-F)\phi_1 \qquad (2)$$

For an intensive quantity, equation 2 can be extended to include the effect of density, ρ :

$$\phi = \left[F\rho_2\phi_2 + (1-F)\rho_1\phi_1\right] / \rho_{mix} \qquad (3)$$

The location of the "anchor point" in the PLIC scheme, (Kothe, et al., 1996), is determined by finding the infinite cutting plane perpendicular to the normal unit of the infinite plane that truncates the correct liquid volume from the cell, i. e., which satisfies the condition.

$$V_{cut} = F V_c \qquad (4)$$

In the PLIC scheme, each cell has a unique normal surface that can be used to compute the surface curvature from cell to cell. This enables the calculation and addition of surface tension forces for the free surfaces. Within each computational cell, the stability limit is given by the so- called Courant Condition:

$$\Delta t_c = \frac{d_c}{|c_c|} \tag{5}$$

The net normal force acting on the surface is equal to the summation of all the tangential forces due to surface tension:

$$\int \Delta p ds = \int \tau |dx| \tag{6}$$

Since the tangential force is equal to

$$\tau = \sigma \vec{n} \times \frac{d\vec{x}}{|d\vec{x}|} \tag{7}$$

this leads to

$$\int \Delta p ds = \int \sigma \vec{n} \times d\vec{x}, \qquad \vec{n} = \nabla F \tag{8}$$

With this free surface simulation in piecewise linear interface Construction (PLIC) method, a two-dimensional Navier-Stokes code (CFDRC, 2000) is used to model the two-phase flow field around the ship spoiler. The computing process can be implemented to find the fluid-fluid interface at each cell, find the unit normal of the interface, then apply the above integral to determine an effective cell volume force. From the pressure distribution upstream, downstream of the spoiler and on the spoiler body the resultant force on the ship bottom and the spoiler is computed. The moment around spoiler fixation is determined which affect the roll, pitch and speed of the ship.

3. Experimental Facility, Methods and Parameters.

The experiments were carried out in a water tunnel facility at the Hydraulic and Turbomachinery Laboratory of the Irrigation Engineering Department at Zagazig University. A schematic of the apparatus construction and water tunnel photo are shown in Figs. 2a and 2.b respectively. The water tunnel test section is 3m long, 0.31 m height and 0.1m width. The pump has a discharge of 10 L/s and power of 2 hp. The width and the depth of water in the water tunnel were ten and five times the spoiler height respectively. The air was injected immediately beside the spoiler, at a distance L downstream the spoiler and at both location at the same time. The two air injectors had a 0.2L inside diameter. The flow rates of the air injectors were kept constant at room temperature and at 6mm water equivalent head. The plate that simulates the ship bottom surface (0.9x 0.1x 0.004 m) is from Plexiglas to allow the light rays to pass through. The spoiler length is 0.01 m. The light source is generated from high power lamp inside a box with a rectangular opening to have parallel light rays. The side of the water tunnel test section is from Plexiglas for flow visualization. The other side and bottom of the text section is painted with black color to prevent light beam reflection. The whole apparatus is set at a dark room to prevent any other light source.

The bubbles growth was recorded with a video camera (Panasonic M9500), which allowed the collection of 30 frames per second. The scientific video recorder (Panasonic- NV-HD100) has 6 heads, which allow the ability for displaying each frame without image noise. The images were digitized with a video capture system in a PC. The results reported here for a Froude number of 1.6 base on spoiler length and the spoiler ship angle (θ) was set to θ=90° and 45°.

4. Grid Structure And Boundary Conditions

The flow is computed for different spoiler inclinations and injection positions. The ship spoiler grids structures are shown in Figs. 3a and 3.b. The grids structure is divided into five 2-D blocks using the multi-block system. Three blocks are under water free surface. The first and second blocks are beside the spoiler and having 93x25, 76x25 grid points, while the third one below the spoiler has 189x50 grid points. The grids are clustered near the spoiler to solve the fluid interaction. The other two 2-D blocks in air represent the injection pipes. The total number of cells is 16349. The total length of the grids in physical domain is about 40L while the depth is 11L as shown in Fig. 3. The two-dimensional Navier-Stokes equations with the free surface simulation in (PLIC) method are discretized on a structured grid using an upwind difference scheme.

The upstream boundary conditions are 5 m/s axial water velocity. The kinematic viscosity of water and air was assumed to be constant. The downstream boundary conditions are atmospheric pressure. The initial injection air velocity is 10 m/s. Fluid in all blocks are starting with water except the two injection pipes are completely full of air at constant temperature 300 K. The physical time step is optimized between $1x10^{-3}$ and $1x10^{-4}$ second for the unsteady flow computations in order to resolve accurately the transients of the cavity formation. The program simulation running time to calculate the development of fluid motion during one-second takes about 32 days (763 hr) on a workstation with double processor Pentium III 450 MHz.

There are three sets of results, which are computed. The first set for an air injection beside a spoiler with θ=90° and 45°. The second for an injection at a distance L and 0.71L from the spoiler with θ=90° and 45° respectively. The third is double air injection beside the spoiler and at a certain distance downstream the spoiler in the same time.

5. Results and Discussion

The transient flow around a ship spoiler is affected by air injection, spoiler position and spoiler inclination. For the above different conditions, the bubbles shape, the two-dimensional flowfield around the spoiler body and the pressure variation on the wake of the spoiler body were determined.

Figure 4 displays the iso-density computational contours for cavities formation in a time sequence beside ship spoiler and the experimental images for the bubble at the same time. The air injection was just beside ship spoiler with spoiler angle (θ) of 90°. The ship spoiler has a length L. The upstream speed (u) equals 5 m/s. The injection velocity (v) of air equals 10 m/s downward. The physical time for each calculating step is optimized at $1x10^{-3}$ s. It is demonstrated that the cavity formation has three stages. First, a cavity starts to grow at the wake of the spoiler body as shown in Figs. 4a-c. At the second stage, the cavity starts to split as shown in Figs. 4d-f. Finally, the splited cavity runs away to collapse at the third stage as shown in Fig. 4g. The cavity is attached to the ship spoiler from the beginning. The computational and experimental results show that there is a good matching of bubble formation except the computational bubble shape has little more depth. This may be due to that the computation was in 2D only.

Figure 5 displays the iso-density computational contours and the experimental images for cavities formation in a time sequence, where air injected at a distance L downstream the ship spoiler at spoiler angle (θ) of 90°. The ship spoiler has length L. The upstream speed (u) equals 5 m/s. The injection velocity (v) of air equals 10 m/s downward. The physical time for each calculating step is optimized at $1x10^{-3}$ s. It is demonstrated that the cavity formation

has three stages till it split and run away. First, a cavity starts to grow downstream of the injection hole as shown in Figs. 5a-b. At the second stage, the cavity starts to grow upstream of the injection hole and attaches the spoiler as shown in Figs. 5c-e due to reverse flow. At the third stage, the cavity splits and the splited cavity runs away to collapse as shown in Figs. 5f-g. The computational and experimental results show that there is a good matching of bubble formation.

Figure 6 indicates the iso-density computational contours and the experimental images for cavities formation in a time sequence, where air injected both beside the ship spoiler and at a distance L downstream the spoiler and spoiler angle (θ) of 90°. The ship spoiler has length L. The upstream speed (u) equals 5 m/s. The injection velocity (v) of air equals 10 m/s downward. The physical time for each calculating step is optimized at $1x10^{-3}$ s. It is demonstrated that the cavity formation has three steps. First, two cavities start to grow separately around the injection holes as shown in Fig. 6a. At the second stage, the cavities merge together and grow downward direction as shown in Figs. 6b-d. At the third stage, the cavity grows mainly downstream and takes the final form as shown in Figs. 6e-g. The bubble growth is more stable and takes the final form more rapidly. The computational and experimental results show that there is a good matching of bubble formation.

Figure 7 shows the iso-density computational contours and the experimental images for cavities formation in a time sequence, where air injected beside the ship spoiler and spoiler angle (θ) of 45°. The ship spoiler has length L. The upstream speed (u) equals 5 m/s. The injection velocity (v) of air equals 10 m/s downward. The physical time for each calculating step is optimized at $1x10^{-4}$ s. It is demonstrated that the cavity formation has three stages. First, a cavity starts to grow at the wake of the spoiler body as shown in Figs. 7a-c. At the second stage, the cavity takes long foot shape as shown in Figs. 7d-e. Finally, the bubble starts to split and run away to collapse at the third stage as shown in Fig. 7f. But, the experimental images show that the bubble was filling the space between the spoiler and the body of the ship. This is may be due to two-dimensional computational model consideration. So, a layer of water was isolated between the bubble and the ship body.

Figure 8 displays the iso-density computational contours and the experimental images for cavities formation in a time sequence, where air injected at a distance 0.71L from ship spoiler and spoiler angle (θ) of 45°. The ship spoiler has length L. The upstream speed (u) equals 5 m/s. The injection velocity (v) of air equals 10 m/s downward. The physical time for each calculating step is optimized at $1x10^{-4}$ second. It is demonstrated that the cavity formation has three stages. First, a cavity starts to grow at the wake of the spoiler body as shown in Figs. 8a-d. At the second stage, the cavity takes long foot shape as shown in Figs. 8e-f. Finally, the bubble starts to split and run away to collapse at the third stage as shown in Fig. 8g. But, the experimental images show that bubble was filling the space between the spoiler and the body of the ship. This is may be due to two-dimensional computational model consideration. So, a layer of water was isolated between the bubble and the ship body.

Figure 9 represents the velocities vectors and density, total pressure and pressure contours around the spoiler of with (θ) 90° and the air injection beside after one second. This flow condition was shown in Fig. 4. The iso-total pressure contours are approximately similar to the iso-density contours. There is a reverse flow between the bubble and the ship surface in the wake region from 2-4L of the spoiler. The maximum velocities are concentrated around the injection hole and spoiler tips. In this case, the maximum/ minimum pressures around upstream/ downstream of the spoiler are about 17173/-18716 N/m^2. The resulting

moment around spoiler fixation point due to fluid interaction in the area of 15L upstream and downstream the spoiler is 172 KN.m.

Figure 10 shows the velocities vectors and density, total pressure and pressure contours around the spoiler with angle (θ) 90° and air injection at a distance L downstream from it after 1.2 second. This flow condition was illustrated in Fig. 5-g. The iso-total pressure contours are approximately similar to the iso-density contours. There is a reverse flow between the bubble and the ship surface in the wake region from 2-3L of the spoiler. The maximum velocities are concentrated around the injection hole and spoiler tips. In this case, the maximum/ minimum pressures around upstream/ downstream the spoiler are about 16378/-25090 N/m^2. The resulting moment around spoiler fixation point due to fluid interaction in the area of 15L upstream and downstream the spoiler is 8.7 times the moment for the condition of injection beside the spoiler.

Figure 11 indicates the velocities vectors and density, total pressure and pressure contours around the spoiler with an angle (θ) 45° and air injection beside it after 1.4 second. This flow condition represents the case shown in Fig. 7-f. The iso-total pressure contours contain the span of the bubble till the ship wall. The flow is circulated inside the bubble. The maximum velocities are concentrated around the injection hole and spoiler tips. In this case, the maximum/ minimum pressures around upstream/ downstream of the spoiler are about 14712/-27688 N/m^2. The resulting moment around spoiler fixation point due to fluid interaction in the area of 15L upstream and downstream the spoiler is 6.7 times the moment for the condition of injection beside the spoiler with 90°.

Figure 12 represents the velocities vectors and density, total pressure and pressure contours around the spoiler with an angle (θ) 45° for the injection at a distance L from it after 1.96 second. This flow condition represents the case shown in Fig. 8-g. The iso-total pressure contours contain the span of the bubble till the ship wall. The flow is circulated inside the bubble. The maximum velocities are concentrated around the injection hole and spoiler tips. In this case, the maximum/ minimum pressures around upstream/ downstream of the spoiler are about 16717.2 / -19490.7 N/m^2. The resulting moment around spoiler fixation point due to fluid interaction in the area of 15L upstream and downstream the spoiler is 15 times the moment of the condition of injection beside the spoiler with 90°. The same resulting moment for the bubble after 1.2 second only is 6.9 times the moment of the condition of injection beside the spoiler with 90°. This means that the bubble size have a great effect upon the pressure and moment around the spoiler.

Figure 13 displays the velocities vectors and density, total pressure and pressure contours around the spoiler with angle (θ) 45° for the double air injection case beside and at a distance L downstream it after 1.2 second. The upstream speed (u) equals 5 m/s. The injection velocity (v) of air equals 10 m/s downward. The physical time step is optimized at $1x10^{-4}$ s. The iso-total pressure contours contain the span of the bubble till the ship wall. The flow is circulated inside the bubble. The maximum velocities are concentrated around the injection hole and spoiler tips. In this case, the maximum/ minimum pressures around upstream/ downstream of the spoiler are about 16506.4/-24613.9 N/m^2. The resulting moment around spoiler fixation point due to fluid interaction in the area of 15L upstream and downstream the spoiler is 7.9 times the moment for the condition of injection beside the spoiler with 90°. This moment becomes 17.8 times the moment around the spoiler with 90° after 2 second.

6. SUMMARY AND CONCLUSIONS

The transit flow around ship spoiler with injection of exhaust gases or air forming

cavity is affected by spoiler position and its inclination angle. This ship spoiler has a strong wake effect with gas injection position, which can control the ship oscillation.

It is demonstrated that the cavity formation has mainly three stages. First, a cavity starts to grow at the wake of the spoiler or downstream. In the second stage, the cavity grows upstream of the injection hole and attaches the spoiler or takes long foot shape (45° spoiler) or the cavities merge together and generate a bubble depth (double injection). In the third stage, the bubble starts to split and the splited cavity runs away to collapse.

The computational and experimental results show that there is a good matching of bubble formation in the spoiler with 90°. This indicates that modeling the two-phase flow field around a ship spoiler using two-dimensional Navier-Stokes with the Free Surface simulation in Piecewise Linear Interface Construction (PLIC) method is successful. In the conditions of 45° the experimental images show that bubbles fill the space between the bubbles and the body of the ship. This is may be due to two-dimensional computational model consideration. So, a layer of water was isolated between the bubble and the ship body.

In the spoiler of 90°, the iso-total pressure contours are approximately similar to the iso-density contours. There is a reverse flow between the bubble and the ship surface in the wake region from 2-3L of the spoiler.

In the spoiler of 45°, the flow is circulated inside the bubble. The bubble shape is longer which gives more negative pressure on larger area. The moment around the fixation point of the spoiler of 45° is higher seven times than that around the spoiler of 90°.

In double injection condition beside and at a distance L downstream from the spoiler, the bubble is stable and has more moment around the spoiler.

Thus, changing inclination spoiler angle and position relative to injection angle will gives different pressures that create forces and moment which can control the roll, pitch motion and speed of the ship.

7. REFERENCES

CFDRC, 2000, "CFD-ACE+ Theory And Users' Manuals Ver.6.4" *CFD Research Corporation*. Huntisville, Al., USA.

Hirt and Nichols, "VOF Method For The Dynamics Of Free Boundaries," *J. Computational Physics*. Vol. 39, 201 (1981).

Kothe, D.B., Rider, W.J, Mosso, S.J., and Brock, J.S.,, 1996, "Volume Tracking Of Interfaces Having Surface Tension In Two And Three Dimensions," AIAA Paper, 96-0859.

Mostafa, N. H., 2001 "Computed Transient Supercavitating Flow Over a Projectile" *Mansoura Engineering Journal, MEJ,* Vol.26 No.2, PP. M79-M91.

Noh, W.F. and Woodward, P.R., 1976, "SLIC (simple line interface method)," In A.I. van de Vooren and P.J. Zandbergen, *Lecture Notes in Physic,*. Vol 59, pp. 330-340.

Soper, R. R., Nayfeh, A. H. and Mook, D. T., 1998, "Control of Rolling Ships By Hull-Mounted Spoilers" *Fourth Semi-Annual Meeting- MURI, Nonlinear Active Control Of Dynamical Systems*. Blacksburg, VA., USA.

Rider and Kothe, 1995, "Stretching and Tearing Interface Tracking Methods" AIAA, 95-1717.

Owis, F., Nayfeh, A. H., and Mook, D. T., 2000 "Control Of Roll Motion Using a System Of Spoilers" *Seventh Semi-Annual Meeting– MURI- Nonlinear Active Control of Dynamical Systems,* Blacksburg, VA, USA.

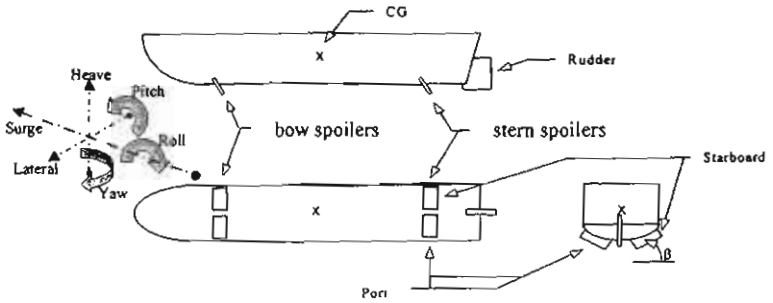

Fig. (1) Example of ship spoiler locations, Soper, et al., 1998.

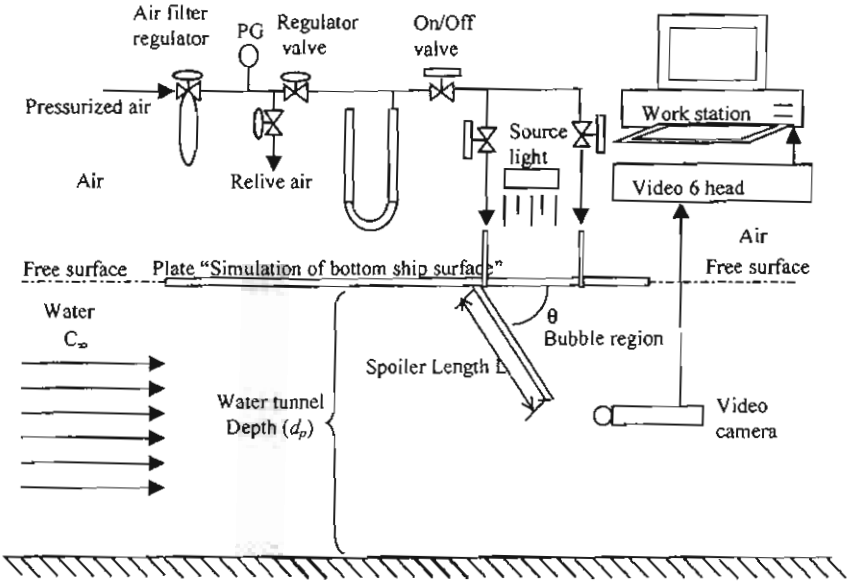

Fig. (2-a) Schematic diagram of the ship spoiler construction and instrumentation.

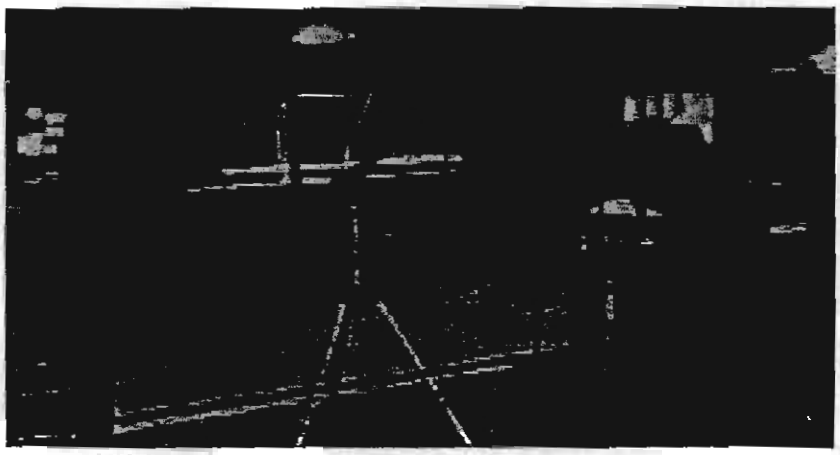

Fig. (2-b) Water tunnel of the ship spoiler and instrumentation.

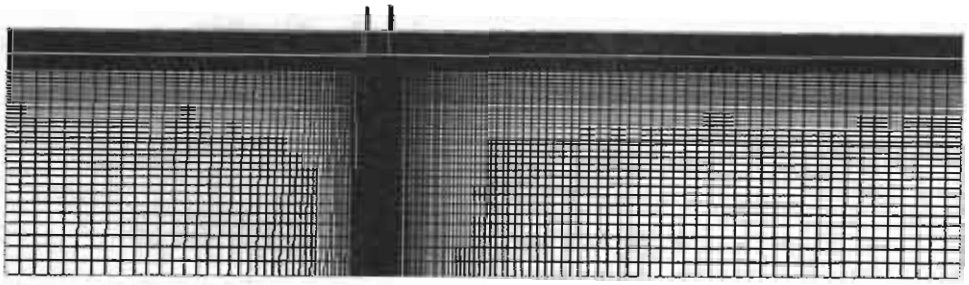

3-a Structured grid of ship spoiler of 90°.

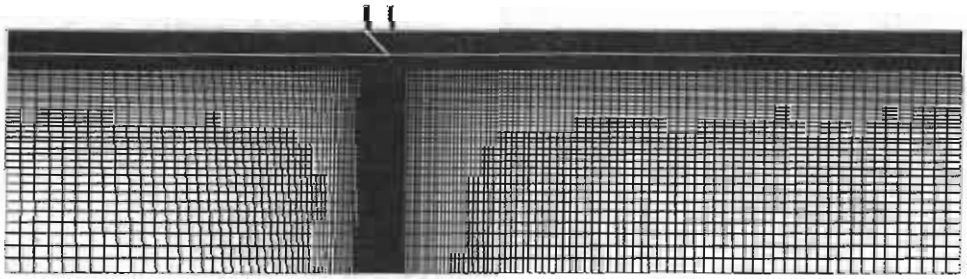

3-b Structured grid of ship spoiler of 45°.

Fig. (3) Grid shape of ship spoiler.

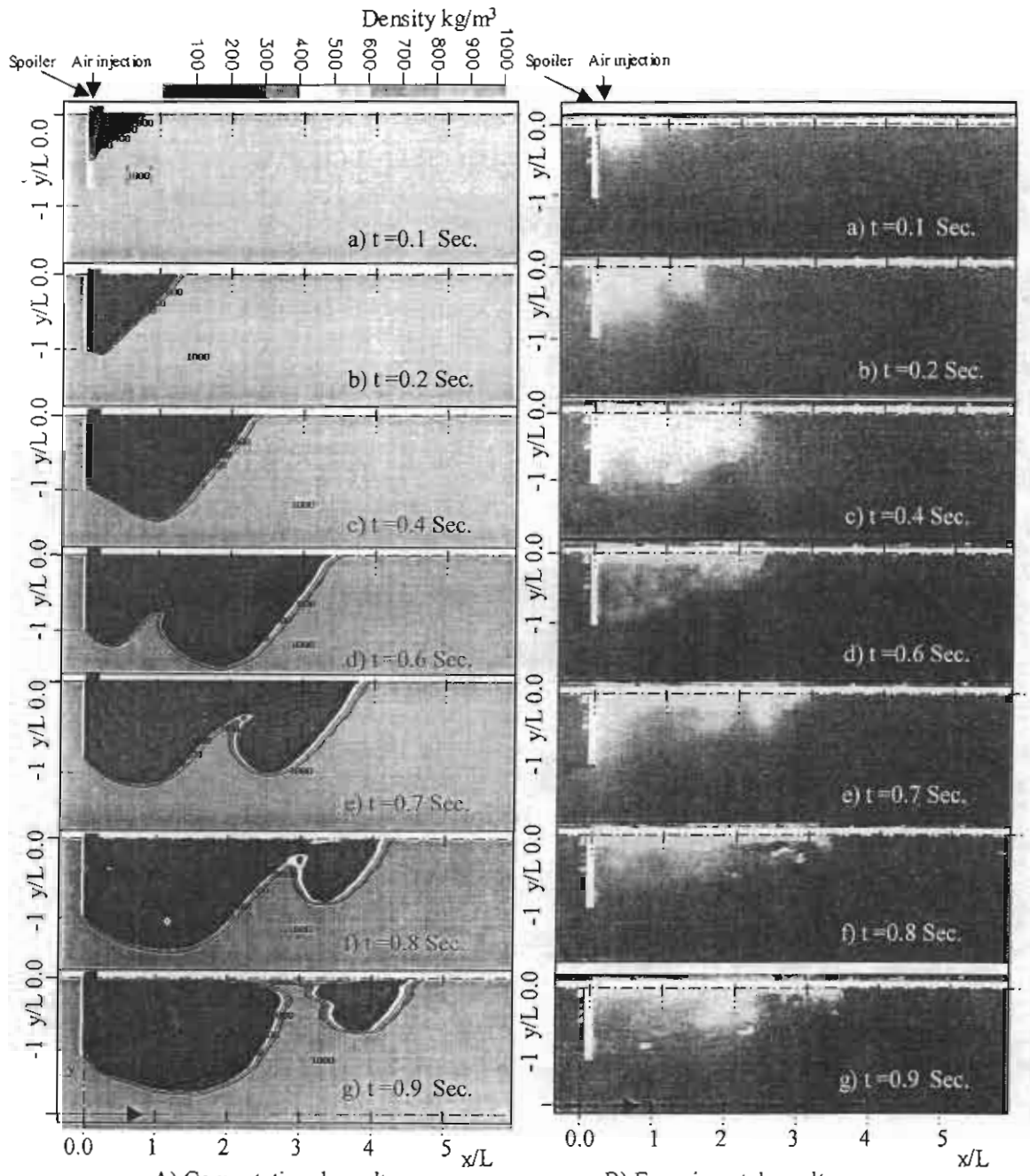

A) Computational results. B) Experimental results.

Fig. (4) Cavities formation due to injection beside spoiler with $\theta=90^{\circ}$.

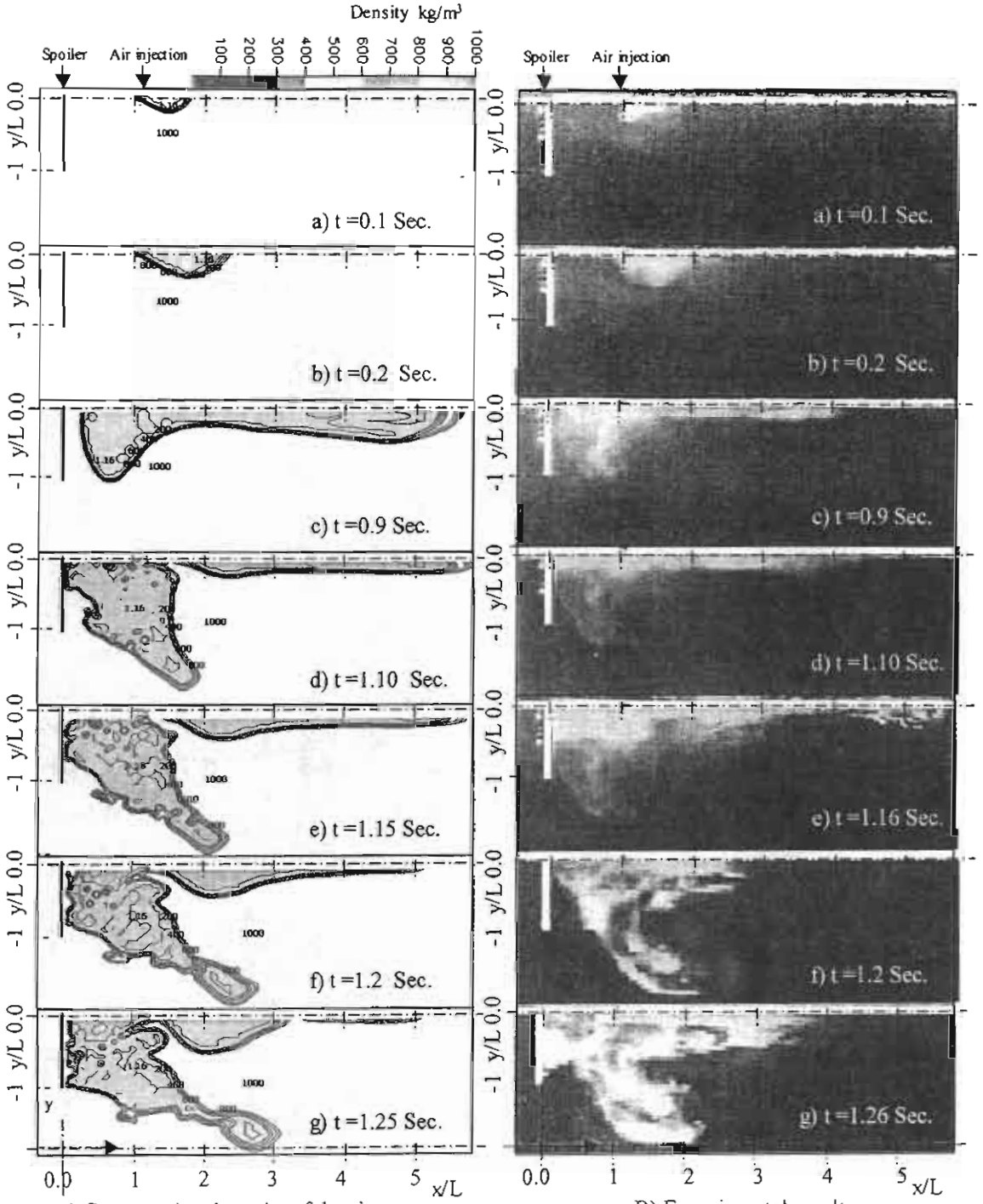

A) Computational results of density contours. B) Experimental results.

Fig. (5) Cavities formation due to injection at a distance L from the spoiler with θ=90°.

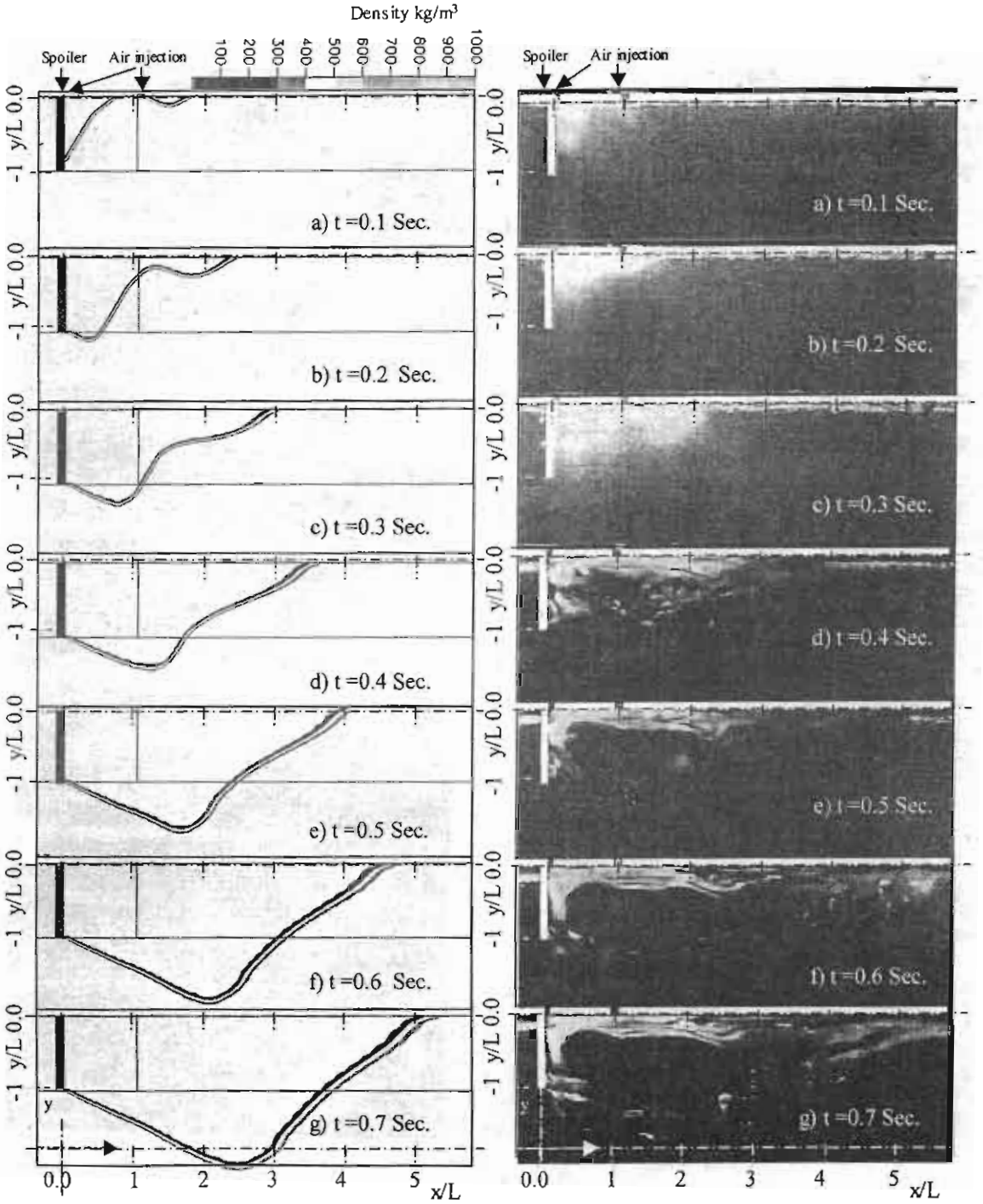

A) Computational results of density contours. B) Experimental results.

Fig. (6) Cavities formation due to double injection beside spoiler and at a distance L from the spoiler with $\theta=90^{\circ}$.

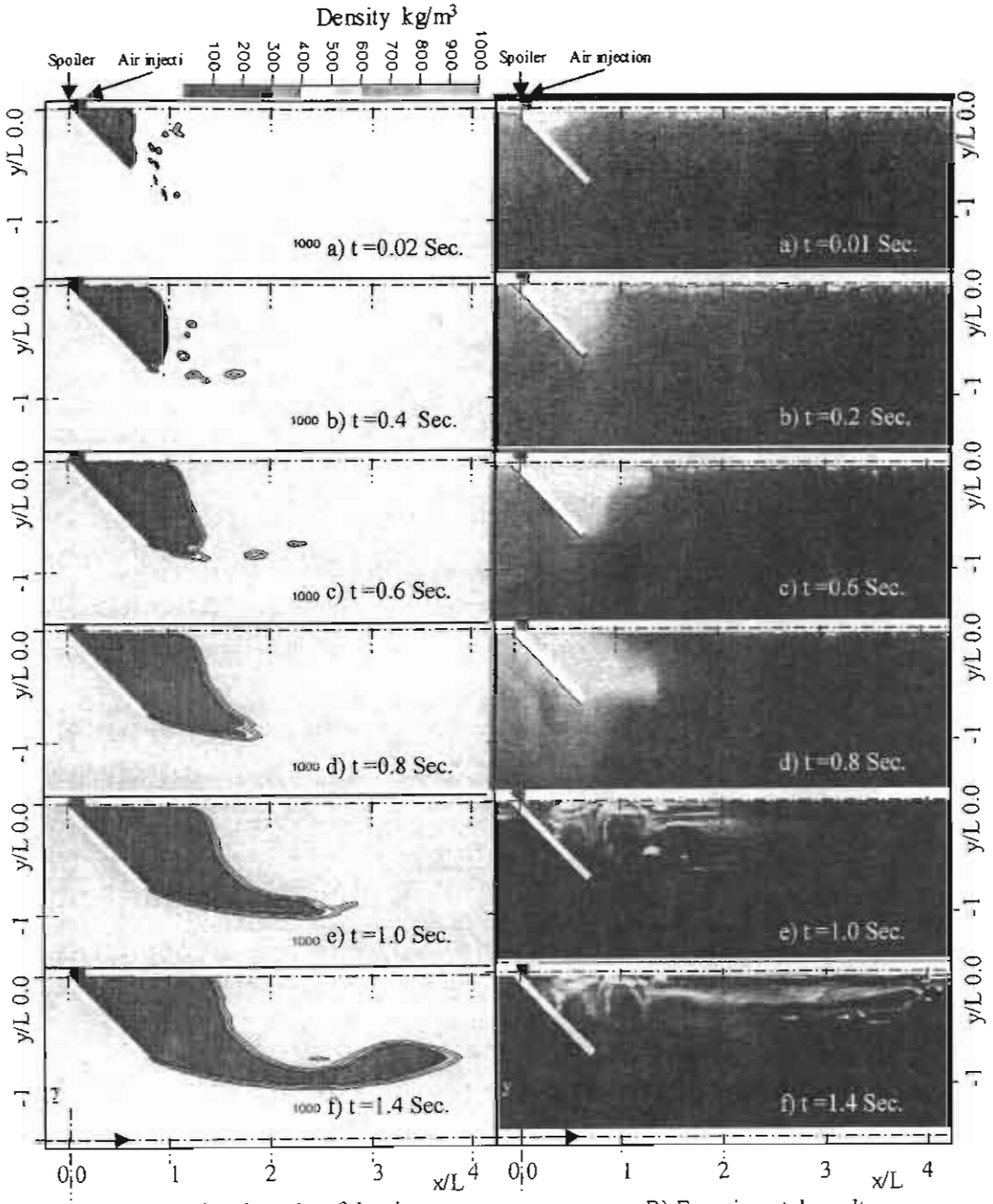

A) Computational results of density contours. B) Experimental results.

Fig. (7) Cavities formation due to injection beside the spoiler with $\theta=45^{o}$.

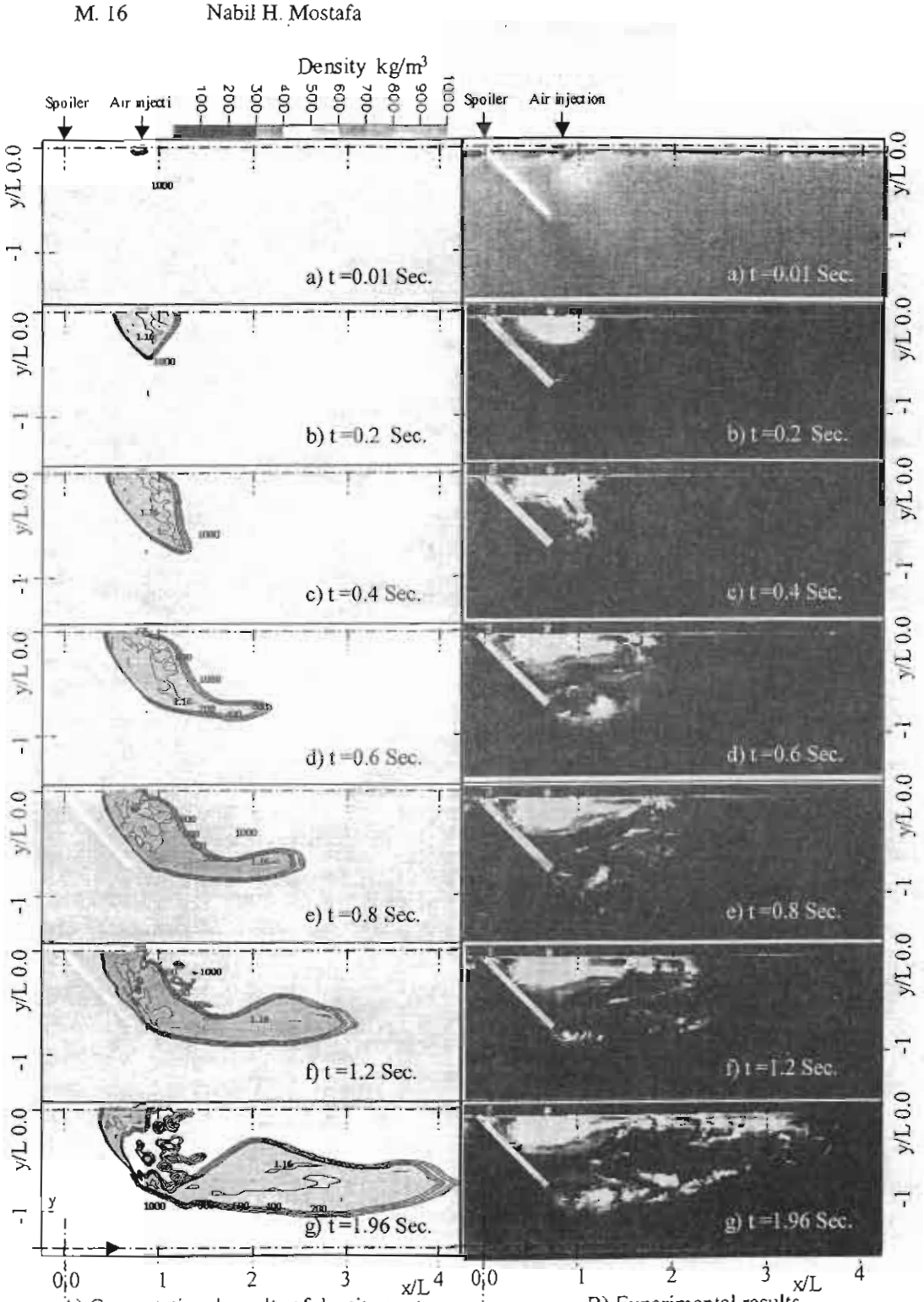

A) Computational results of density contours. B) Experimental results.

Fig. (8) Cavities formation due to injection at a distance L from the spoiler with $\theta=45^{\circ}$.

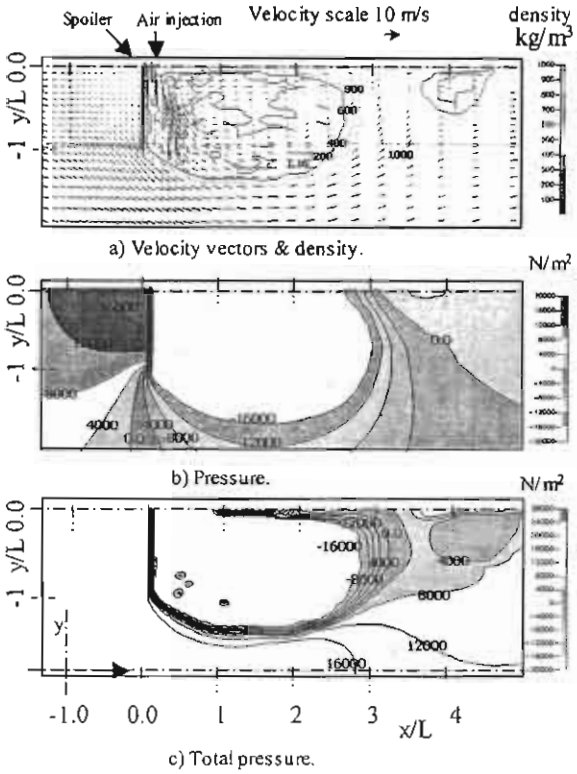

Fig. (9) Flow condition due to injection beside the spoiler with θ=90°, u=5 m/s and t=1Sec.

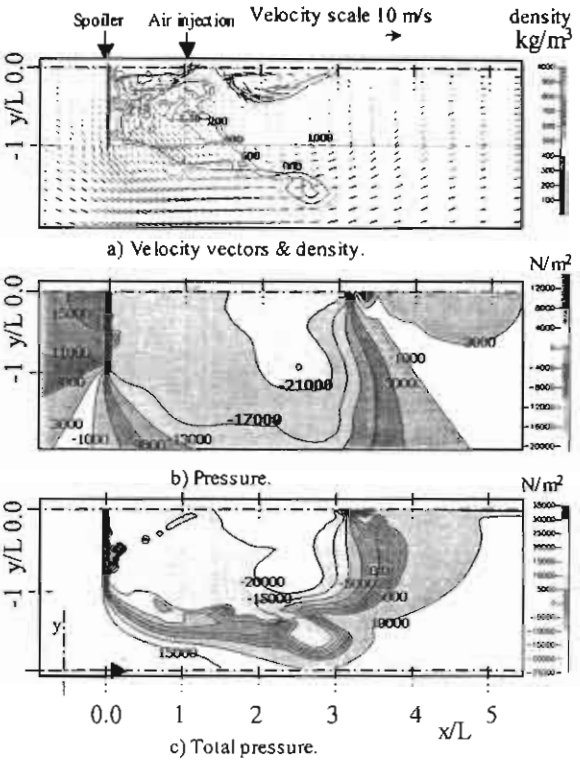

Fig. (10) Flow condition due to injection at a distance L from the spoiler with θ =90°, u=5 m/s and t= 1.25 sec.

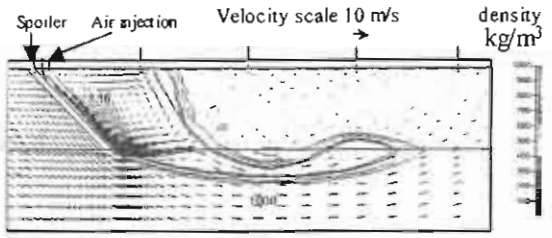

a) Velocity vectors & density.

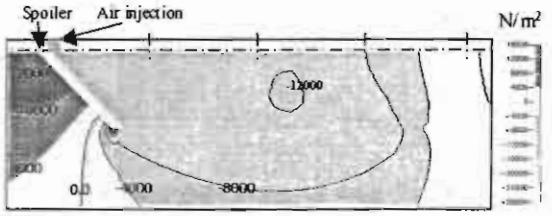

b) Pressure.

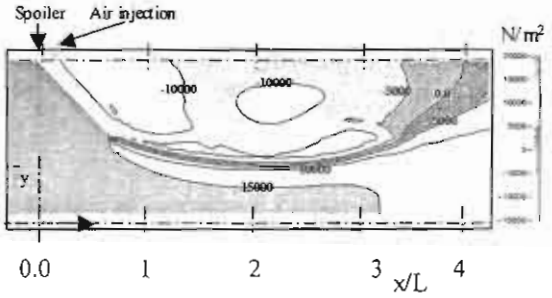

c) Total pressure.

'ig. (11) Flow condition of injection beside the spoiler with θ =45°, *u*=5 m/s and t= 1.4 sec.

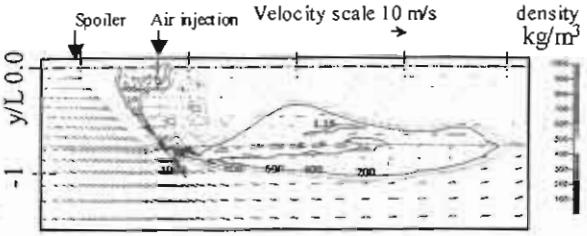

a) Velocity vectors & density.

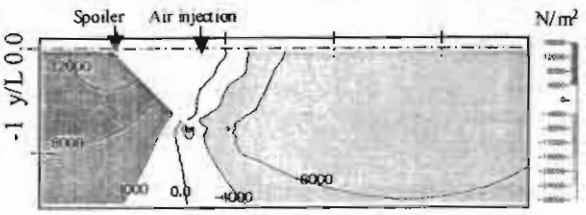

b) Pressure.

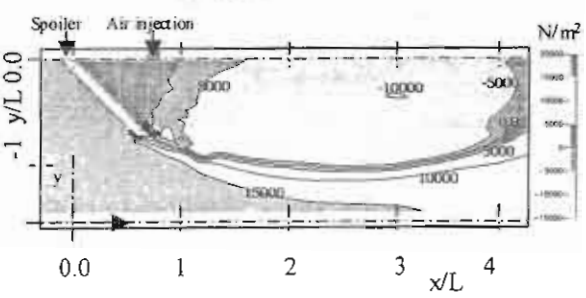

c) Total pressure.

Fig. (12) Flow condition due to injection at a distance 0.71L from the spoiler with θ =45°, *u*=5 m/s and t= 1.96 sec.

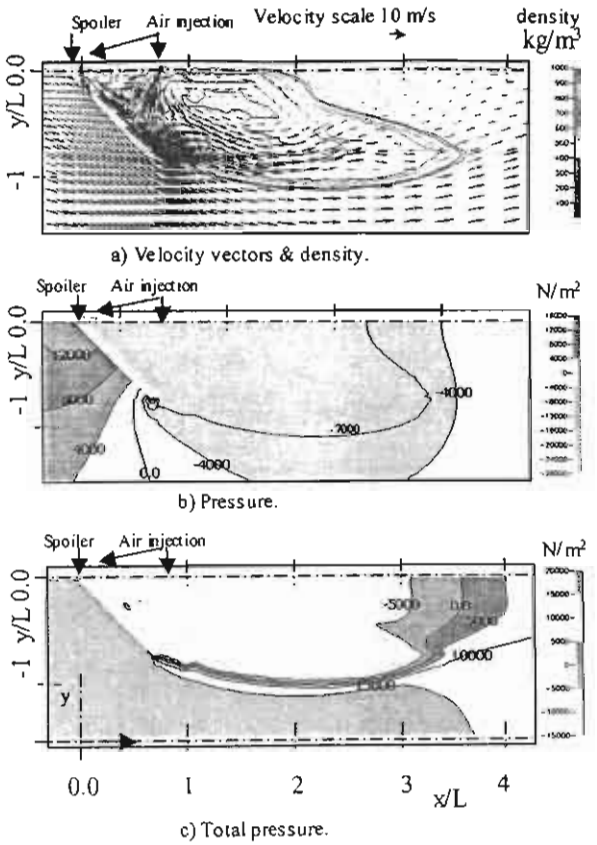

Fig. (13) Flow condition at injection both beside the spoiler and at a distance 0.71L from the spoiler with $\theta = 45^{\circ}$ and t= 1.2 sec.